

Do we need to recourse to Ampère-Neumann electrodynamics to explain wire fragmentation in the solid state?

A. Lukyanov, S. Molokov

Coventry University, School of Mathematical and Information Sciences, Priory Street,
Coventry CV1 5FB, U.K.

Abstract

Exploding wires are widely used in many experimental setups and pulsed power systems. However, many aspects of the process of wire fragmentation still remain unclear. If the current density is not too high, the wire may break up in the solid state. The experiments have shown that the wires break in tension due to longitudinal forces of unknown nature.

In a series of papers, see [2, 3, 4, 5] Graneau argued that neither mechanical vibrations induced by the electromagnetic pinch force nor thermal expansion could have been responsible for the wire disintegration because they were too weak. To explain the phenomenon he appealed to the obsolete Ampère force law as opposed to the conventional Biot-Savart force law. Graneau argued that the Ampère force law would lead to a longitudinal tension in the wire, although his calculations may have been in error on this point. Therefore, Graneau's explanations induced a controversy in electrodynamics with a number of authors arguing *pro* and *con*.

Previous theoretical and numerical investigations served to provide a search for these forces without recourse to unconventional electrodynamics have identified the pinch effect and thermal expansion as a source of strong longitudinal vibrations. But the tensile stress component has been proved to be present only in the wires having free ends. Thus the mechanism doesn't give a satisfactory explanation of the phenomenon in the wires with clumped ends. In this investigation, we use a simplified magneto-thermo-elastic model to study flexural vibrations induced by high pulsed currents in wires with clumped ends on account of their role in the disintegration process. Several aspects are studied, namely (i) the buckling instability due to simultaneous action of the thermal expansion and the magnetic force, (ii) the flexural vibrations induced in initially bent wires. It is shown that the induced flexural vibrations are strong enough to lead to the breaking of the wire in a wide range of parameters.

1 Introduction

The phenomenon of wire fragmentation in the solid state by high pulsed currents was studied experimentally by Nasilowski [1], and Graneau [2, 3, 4]. They observed that a sufficiently strong electric current would shatter a thin metal wire under a broad range of conditions (various wire material and geometry, different current types, etc.). As a result of the explosion the wires fragmented into 2-100 pieces with apparent signs of longitudinal tensile stress.

The experimental results, as well as (sometimes controversial) early attempts to explain the phenomenon have been reviewed by Graneau [5], Hong [6] and Molokov&Allen [7].

It is obvious that an electric current passing through a metal wire induces stress waves. Their origins are in (i) the thermal expansion owing to the volumetric Joule heating, and (ii) the Lorentz-, or pinch-, force. These forces depend on the magnitude and the rate of change of the current passing through the wire. They grow as either of these parameters increases.

Ternan [8] suggested that in Graneau's experiments with wires with free ends standing stress waves may be induced as a result of thermal expansion. Using a simple one-dimensional model he showed that the resulting stresses were sufficient to lead to a fracture.

This mechanism of fragmentation of wires with free ends has been explored in more detail by Molokov&Allen in [7]. They employed a magneto-thermo-elastic model of the stress-wave propagation, and solved the problem numerically on assumption of axisymmetric nature of vibrations. Their conclusion was that the characteristic value of both compressive and tensile longitudinal stresses obtained for the aluminium wire with radius $a = 0.6$ mm carrying current $I = 5$ kA and having free ends (the parameters relevant to the experiment in [3]) would be about 33 MPa per unit length of the wire. The stress has been shown to grow linearly with the wire length and thus, for sufficiently long wires, the resultant stress exceeds the ultimate strength of aluminium. This is 75 MPa at 100° C going down to 17 MPa at 320° C [9].

Although the mechanism does give large value of tensile stresses, it cannot explain the fragmentation of wires with clamped ends (as in the experiments [1, 4]) because within the axisymmetric model in this case the stresses can be only compressive [7]. It is clear, however, that in the wires with clamped ends flexural vibrations may be induced. The apparent signs of these modes have been observed in the Graneau's experiments on the wires with firmly clamped ends. The resultant wire shape, after breaking, clearly indicated on that, see photographs in [4].

In this paper we carry out a special study of flexural vibrations to account for their role in fragmentation of wires with clamped ends. In section 2, we present the formulation of

the problem and discuss simplifications of the model. In section 3, the linear stability of the system is considered. In section 4, we carry out a qualitative analysis of expected stresses. In section 5, numerical algorithm and results are presented.

2 Formulation

Consider a wire which is firmly clamped between two points located along the z -axis. Let the distance between these points be L . We restrict our attention to the case of plane motion, and denote the deflection of the wire from the axis by X which is a function of z and time t . The deflection of the wire in the initial undeformed state is denoted by X_0 . Possible three-dimensional modes, not considered here, may only increase stresses, especially at the clamped ends.

Our theoretical consideration is based on a simplified model valid for sufficiently long or sufficiently thin wires. In this model the deflection X of the wire is assumed to be much lower than the wire length, i.e. $|X|/L \ll 1$. Since large deflections of the order of the wire length are not expected in the wire explosion experiments, this restriction is not expected to be very stringent. Another small parameter used in the model is the ratio $a/L \ll 1$, where a is the wire radius. This condition is usually well satisfied. Plastic deformations are not considered here although they may be important in the vicinity of the melting point. Thus all deformations are assumed to be elastic.

Then the deflection X obeys the following equation ([10]):

$$\rho S \frac{\partial^2 X}{\partial t^2} + E \frac{\partial^2}{\partial z^2} J \frac{\partial^2 X}{\partial z^2} - E \frac{\partial^2}{\partial z^2} J \frac{\partial^2 X_0}{\partial z^2} - G \frac{\partial^2 X}{\partial z^2} - F_x - \frac{\partial C_y}{\partial z} = 0 \quad (1)$$

where ρ is the material density, S is the wire cross-section which may be a function of z , J is the effective moment of inertia of the wire cross-section (for a circular cross-section $J = \pi a^4/4$, where a is the wire radius), E is the Young modulus, G is the force along the z axis applied at the wire ends, F_x is the distributed external force per unit length along the x direction and C_y is the distributed moment of force along the y direction per unit length.

For the physical situation considered here, the force G can be represented as

$$G = ES\{(\tilde{l} - \tilde{l}_0)/L - \alpha[T(t) - T_0]\},$$

The second term is a compressive force due to the thermal expansion, α being the linear expansion coefficient. The first, nonlinear term is a retarding force due to the wire deformation from the initial state, where

$$\tilde{l} - \tilde{l}_0 = \frac{1}{2} \int_0^L \left(\frac{\partial X}{\partial z} \right)^2 - \left(\frac{\partial X_0}{\partial z} \right)^2 dz \quad (2)$$

is the increment of the wire length due to the deflection. When $X = X_0$, $\tilde{l} = \tilde{l}_0$ and the retarding force equals to zero, as required.

The boundary conditions are those for the clamped ends, namely

$$X = \frac{\partial X}{\partial z} = 0 \quad \text{at } z = 0 \text{ and } z = L. \quad (3)$$

The initial conditions are

$$X = X_0 \quad t = 0. \quad (4)$$

2.1 The magnetic force

In long, thin wires under consideration $a/L \ll 1$, uniform current is directed perpendicular to the cross-section. Thus any possible forces of magnetic nature act only in the cross-section plane. These forces create no moment and thus $C_y = 0$ in our case.

The net distributed force \mathbf{F} can be calculated directly from

$$\mathbf{F} = \int \mathbf{j} \times \mathbf{B} dS. \quad (5)$$

The integral in (5) is taken over the wire cross-section area. The magnetic field is given by the Biot-Savart law

$$\mathbf{B} = \frac{\mu_0}{4\pi} \int \frac{\mathbf{j} \times \mathbf{R}}{\mathbf{R}^3} dV', \quad (6)$$

where dV' is the volume element on the wire, \mathbf{j} is the current density, and the vector $\mathbf{R} = \mathbf{r} - \mathbf{r}'$ is directed to the field point as usual.

To calculate the x component of the force, F_x , one can split the integral (6) over the wire length z' into two parts $\mathbf{B} = \mathbf{B}_{\text{in}} + \mathbf{B}_{\text{ex}}$. The first part of the integral \mathbf{B}_{in} is taken over the

range $|z' - z| < \Delta$, where $a \ll \Delta \ll \xi_L$, ξ_L being the characteristic length scale of the function $X(z)$. The second part \mathbf{B}_{ex} is taken over the rest of the wire length $\Delta < |z' - z| < L$, whereby the volume integral reduces to the integration over the wire length only. That is,

$$\mathbf{B}_{\text{ex}} = \frac{\mu_0}{4\pi} \int \frac{\mathbf{I} \times \mathbf{R}}{\mathbf{R}^3} dl',$$

where I is the total current. The first integral can be evaluated in general with the assumption of a uniform current distribution and in the approximation $a \ll \xi_L$, $|X|/\xi_L \ll 1$. The first inequality has been implicitly introduced in fact when we set the length Δ , the second inequality just represents the fact that the wire is slightly deflected from a straight line. The first integration asymptotically gives the expression for the net force as follows

$$\{F_x\}_{in} = -\frac{\mu_0 I^2}{4\pi} \frac{\partial^2 X}{\partial z^2} \{\ln(2\Delta/a) - 3/4\} + O((X/\xi_L)^2, \Delta/\xi_L, (a/\Delta)^2). \quad (7)$$

That is the force is proportional to the local wire curvature [11]. The second part cannot be integrated in a general case and one needs to make certain assumptions about the wire form and thus about the function $X(z)$ itself. In the case of an infinitely long wire with periodic lateral perturbations $X = \tilde{X} \cos(kz)$, $k = 2\pi/\xi_L$, one gets

$$\{F_x\}_{ex} = -\frac{\mu_0 I^2}{4\pi} \frac{\partial^2 X}{\partial z^2} \{-C + 1/2 - \ln(k\Delta)\} + O(k\Delta, (X/\xi_L)^2, (a/\Delta)^2), \quad (8)$$

where $C \simeq 0.577$ is the Euler's constant and we have substituted $Xk^2 = -\frac{\partial^2 X}{\partial z^2}$. Combining two parts we obtain

$$F_x = -\frac{\mu_0 I^2}{4\pi} \frac{\partial^2 X}{\partial z^2} \{\ln(2/ka) - C - 1/4\}. \quad (9)$$

Note, that the expression (9) is identical to the formula obtained in [12] in a particular case of small periodic deflections $|X| \ll a$.

It is clear that the assumption of an infinitely long wire to calculate the force, F_x , is not very rigorous, since in experiments the circuit is always closed. This implies that in addition to the magnetic force by the wire current itself, there may be a component generated by the currents flowing in the external circuit. This effect can be taken into consideration by substituting an appropriate circuit form, in other words the function $X(z)$ in the second integral.

Alternatively, this force can be obtained by means of the virtual work principle. To estimate how strong the effect could be, we will use a general expression for the inductance of a closed circuit $\Lambda = \frac{\mu_0}{2\pi} L_s \ln(L_s/a_s)$, where L_s is the circuit characteristic length and a_s is the radius of the circuit wire, see [13]. Then varying the circuit length L_s one can calculate the subsequent variation of the associated magnetic energy $E_m = \frac{1}{2} \Lambda I^2$. Then, equalising the net force acting on the circuit F_N with the variation of the energy we get

$$F_N \delta L_s = \frac{\mu_0}{4\pi} I^2 (\ln(L_s/a_s) + 1) \delta L_s. \quad (10)$$

An average force acting on a unit length is $f = F_N/L$. Then, for the average force from (10) we get $f \simeq \frac{\mu}{4\pi_0} I^2 (\ln(L_s/a_s) + 1)/L_s$. The first, logarithmic part of the net force represents contribution from the end effects, see (7). The second part gives the integrated force from the circuit as a whole. If $L \ll L_s$, one can assume that the force is constant throughout the wire length in the first approximation. Then, this "constant" force acting on a wire of length L will create longitudinal stress $\sigma_{\parallel} = \frac{\mu_0^2 I^4}{60480} \frac{\ln(L_s/a_s)^2}{E(\pi a^2)^4} \frac{L^6}{L_s^2}$, see the problem in [10] on page 93. For a copper wire with $L = 30$ cm, $a = 0.6$ mm and the circuit with $I = 5$ kA, $L_s = 20$ m and $a_s = 1$ cm the stress is amounting to $\sigma_{\parallel} \simeq 8.4$ MPa. This is only an estimation, and the effect needs special analysis since the geometry of external circuits is usually unknown. Moreover, using a symmetrical circuit with two loops from both sides of the wire one can completely compensate the external magnetic force.

We leave this question for further detailed investigation and neglect the contribution from the external circuit in our analysis. Further we will use formula (9).

2.2 The temperature behaviour

The temperature behaviour with time is governed by the passing current. It can be calculated according to the direct Joule heating of the wire material from

$$\rho c_v \frac{\partial T}{\partial t} = j^2 / \sigma, \quad (11)$$

neglecting by the process of thermal conductivity. This assumption would hold for thermally isolated wires with uniform current distribution. In expression (11), j is the current density,

ρ and σ are the density and the electrical conductivity of the metal, c_v is the specific heat. From the above equation using the well-known inverse dependence of the conductivity on temperature $\sigma = \sigma_0 \frac{T_0}{T}$ one can obtain

$$T = T_0 \exp(\gamma_T \int_0^t f(t')^2 dt'),$$

where $\gamma_T = \frac{j_0^2}{\sigma_0 T_0 \rho c_v}$ is the characteristic temperature rise-time, j_0 is maximum current density. The function $f(t)$ defines current rise time profile.

3 Linear stability

To investigate possible instabilities in the system, we first carry out a linear stability analysis assuming for a moment that all the parameters, such as current and wire temperature, are constants independent of time. Even though, in a real situation, they vary quite fast with time and numerical methods must be involved to solve the system, our simplified analysis will form a basis for qualitative interpretation and understanding of the results.

3.1 Stability of an initially straight wire

Consider an initially straight wire by letting $X_0 = 0$. General analysis of the system (1) shows that two basic types of buckling instabilities may develop. They are due to thermal expansion, expressed by the force G applied at the wire ends [10], and the magneto-elastic buckling instability [14] expressed by force F_x . In both cases, the instability has a threshold character. When either the force G or the current I exceed some critical value, new stable states appear. The initially stable state $X = 0$ then becomes unstable and buckling occurs.

We are looking for non-trivial stationary solutions of the linearized system (1), (3), (4). They are given by the equation

$$EJX^{IV} - GX'' - F_x = 0, \quad (12)$$

with the boundary conditions

$$X = X' = 0 \quad \text{at } z = 0 \text{ and } z = L. \quad (13)$$

Here, the temperature, T , and the total current, I , are assumed to be independent of time, and so are the functions $G = -\alpha E S[T - T_0]$ and $F_x = -\frac{\mu_0 I^2}{4\pi} X'' \{\ln(2/ka) - C - 1/4\}$.

To obtain a solution to (12) it is convenient to use a complete set of orthogonal functions $\{\mathcal{X}_i\}$, $i \geq 1$ defined by the problem

$$\begin{aligned} \mathcal{X}_i^{IV} + \lambda_i^2 \mathcal{X}_i'' &= 0 \\ \mathcal{X}_i'(0) = \mathcal{X}_i'(L) = \mathcal{X}_i(0) = \mathcal{X}_i(L) &= 0 \end{aligned} \quad (14)$$

with the orthogonality given by

$$\begin{aligned} \int_0^L \mathcal{X}_i'' \mathcal{X}_k'' dz &= \begin{cases} 0, & i \neq k \\ \frac{\lambda_i^4}{2} L, & i = k \end{cases} \\ \int_0^L \mathcal{X}_i' \mathcal{X}_k' dz &= \begin{cases} 0, & i \neq k \\ \frac{\lambda_i^2}{2} L, & i = k \end{cases} \end{aligned} \quad (15)$$

This set of functions is commonly used in the theory of stability and buckling of elastic columns [15].

The eigenvalues of the boundary-value problem (14) satisfy the dispersion equation

$$1 - \cos(\lambda_i L) = \frac{\lambda_i L}{2} \sin(\lambda_i L) \quad (16)$$

So, one can see that the set of functions consists of two subsets. The first subset is defined by the eigenvalues given by

$$\begin{aligned} \cos(\lambda_i L) &= 1 \\ \sin(\lambda_i L) &= 0. \end{aligned} \quad (17)$$

That is

$$\lambda_i = \pi \cdot (i + 1)/L, \quad i = 1, 3, 5, \dots$$

In this case the associated eigenfunctions are given by

$$\mathcal{X}_i = \cos(\lambda_i z) - 1. \quad (18)$$

And the second subset is defined by

$$\begin{aligned} \cos(\lambda_i L) &= \frac{4 - (\lambda_i L)^2}{4 + (\lambda_i L)^2} \\ \sin(\lambda_i L) &= \frac{4\lambda_i L}{4 + (\lambda_i L)^2}. \end{aligned} \quad (19)$$

The associated eigenfunctions are given by

$$\mathcal{X}_i = \cos(\lambda_i z) - 1 + 2z - \frac{2}{\lambda_i L} \sin(\lambda_i z). \quad (20)$$

The first eigenvalue of this subset is equal to $\lambda_2 = 8.986819/L$. Further eigenvalues are approximately given by $\lambda_i \simeq \pi \cdot (i + 1)/L$, $i = 4, 6, 8, \dots$

Now, with the help of (15) one can obtain from (12) a criterion when the instability first appears

$$\alpha(T - T_0)ES - \frac{\mu_0}{4\pi} I^2 (\ln(\lambda_1 a) + 0.14) > EJ\lambda_1^2. \quad (21)$$

The first term on the left hand side of (21) is responsible for the thermal expansion effect, while the second term represents magneto-elastic buckling. It should be noted that while we are considering both effects simultaneously, for parameters relevant to wire explosion experiments these terms have different orders of magnitude.

The criterion obtained shows when the first eigenmode of (1) and the system as a whole become unstable, $\lambda_1 = 2\pi/L$ being the corresponding eigenvalue. In a similar manner, substituting other eigenvalues λ_i for λ_1 , one can obtain respective criteria for higher modes as well.

The set (14) being very useful in the linear stability analysis of system (1) doesn't seem to be very relevant to study the increments of the instability since

$$\int_0^L \mathcal{X}_i \mathcal{X}_k dz \neq 0, \quad i \neq k.$$

But, it would be interesting to obtain an estimate of the increments of the instability. For this purpose, we will substitute a solution to (1) in the form $X = A_i(t)X_i$, i.e. assuming that only one mode is present. Then, for the increment γ_i , ($A_i(t) \sim \exp(\gamma_i t)$), one gets

$$\gamma_i^2 = \frac{E}{\rho} \frac{\lambda_i^2}{2} \frac{L}{\int_0^L X_i^2 dz} \left\{ \Xi - \lambda_i^2 \frac{J}{S} \right\} \quad (22)$$

$$\Xi = \alpha(T - T_0) - \frac{\mu_0 I^2}{4\pi E S} \{0.14 + \ln(a\lambda_i)\}$$

or since $\int_0^L X_i^2 dz \simeq L$

$$\gamma_i \simeq \sqrt{\frac{E}{\rho}} \lambda_i \left\{ \Xi - \lambda_i^2 \frac{J}{S} \right\}^{1/2} \quad (23)$$

As is seen from (23), the increment has a maximum at $\lambda_i = \lambda_{ext}$ defined by the equation

$$\lambda_{ext}^2 = \frac{S}{J} \frac{\alpha(T - T_0)}{2} - \frac{\mu_0 I^2}{8\pi E J} \{0.64 + \ln(a\lambda_{ext})\}. \quad (24)$$

As we will see further, for the range of parameters used in the wire explosion experiments, the contribution from the terms due to magnetic force can be neglected during the initial stage and within this approximation, using explicitly $J = \pi a^4/4$ and $S = \pi a^2$,

$$\lambda_{ext} = \sqrt{\frac{2\alpha(T - T_0)}{a^2}}. \quad (25)$$

And, since $\lambda_i \simeq \pi \cdot (i + 1)/L$,

$$i_{ext} = \sqrt{\frac{2\alpha(T - T_0)}{a^2}} \frac{L}{\pi} - 1. \quad (26)$$

On the other hand, the maximal λ_{lim} at which instability may exist is obtained from (23) to give

$$\lambda_{lim} \simeq 2\sqrt{\frac{\alpha(T - T_0)}{a^2}} \quad (27)$$

with the same accuracy. From (27), since $\lambda_i \simeq \pi \cdot (i + 1)/L$, one gets for the maximal mode number

$$i_{lim} \simeq 2\sqrt{\frac{\alpha(T - T_0)}{a^2}} \frac{L}{\pi} - 1 \quad (28)$$

Thus the dominant mode lies somewhere between the first unstable mode and the last one with the maximal increment

$$\gamma_{ext} = \sqrt{\frac{E}{\rho}} \frac{\alpha(T - T_0)}{a}. \quad (29)$$

From the expression (26) one can see that higher modes are likely to become dominant in the instability spectrum with increase in the wire length. As a result, the wire shape can take a rather intricate form. It seems that the instability on higher modes has been observed experimentally by Graneau, [4]. At the experimental conditions he used, i.e. aluminium wire, $L = 1$ m, $a = 0.6$ mm, from (25) one gets $\lambda_{ext} \simeq 294$ or the corresponding mode number $i_{ext} = 93$ at $T = T_{melt}$. The photographs of the wire shape after the current had been switched off showed clearly the appearance of at least 5 bulges on a small part of the wire.

We will refer further to the sets of parameters presented in Table I corresponding to different wire lengths and different currents. One should note that two sets, [B] and [E], are relevant for wires and currents used in the experiments [4] and [1] respectively.

Table.I

	material	a	L	I	P_1	P_2	P_3
A	aluminium	0.6 mm	0.05 m	5 kA	1.19×10^3	6.11	114
B	aluminium	0.6 mm	1 m	5 kA	1.19×10^3	13.6	0.28
C	aluminium	0.6 mm	1 m	2 kA	1.19×10^3	2.18	0.28
D	aluminium	0.6 mm	0.3 m	8 kA	1.19×10^3	34.8	0.28
E	copper	0.5 mm	1 m	500 A	1.84×10^3	0.14	0.24

For all the represented sets, the criterion (21) is fulfilled well enough. Indeed, we have put in the Table I the corresponding values of the terms in (21), designating them as P_1 , P_2 and P_3 from left to right. The estimations have been done at $T = T_{melt}$, T_{melt} being the melting temperature; $T_{melt} = 660^\circ\text{C}$ for aluminium and $T_{melt} = 1085^\circ\text{C}$ for copper. The characteristic increment (29) at the same conditions, in the case [B] for instance, is $\gamma_{max} \simeq 10^5 \text{ sec}^{-1}$, which is much greater than the temperature increment $\gamma_T \simeq 7 \times 10^2 \text{ sec}^{-1}$. Thus, even though the estimation has been done in the linear approximation, it is clear that the instability has sufficient time to develop before the wire reaches the melting point.

In all the cases, as is seen, the major contribution is from the thermal expansion effect, while the influence of the magnetic-force terms can be neglected during the initial stage (this, of course, can be estimated directly from (1) as well). Two terms, P_1 and P_2 , for instance in case [B], become equal only at $T - T_0 = 6.6^\circ\text{C}$. The time it takes for the temperature to be driven through this range is $\Delta t \simeq 30 \mu\text{sec}$. The characteristic time for the instability to develop for this temperature difference is much longer, $\gamma_{max}^{-1} = 800 \mu\text{sec}$.

3.2 Stability of an initially bent wire

Consider a wire which has an initial form $X_0 = \sum_i A_i^0 \mathcal{X}_i$, where the functions $\{\mathcal{X}_i\}$ is the set (14) and A_i^0 are given weight coefficients. One needs to stress, that with the accuracy the system (1) was derived, $|X_0| > a$ must always be the case. Performing analysis similar

to that leading to equation (21) and neglecting the magnetic force for the sake of simplicity, for a mode k one gets

$$\lambda_k^2(A_k - A_k^0)EJ - A_kES(\alpha\Delta T) = 0. \quad (30)$$

From (30) one can see that there is always a stationary state which differs from X_0 at any nonzero value of the parameter $\alpha\Delta T$. Thus, those modes which have $A_k^0 \neq 0$ are always unstable. The result is not surprising, since from the physical point of view it is obvious that a constantly heated wire will change its form owing to expansion. On the other hand, those modes which have $A_k^0 = 0$ become unstable at some value of the parameter $\alpha\Delta T$, so that buckling instability is still possible on these modes.

4 Qualitative stress analysis.

Once the instability occurs, all the potential energy comprised into the compressed wire can be quickly released. The characteristic value of the longitudinal stress τ_{zz} which may be accumulated during the preconditioning is within the interval between the maximum value $\tau_{zz}^{max} = \alpha(T_{melt} - T_0)E \sim 10^3$ MPa and the minimum value $\tau_{zz}^{min} = E\frac{J}{S}\lambda_0^2 \simeq 0.3 \div 30$ MPa corresponding to the onset of the instability. The estimation has been done for an aluminium wire of radius $a = 0.6$ mm and the length spanning the range $1 \text{ m} > L > 0.05 \text{ m}$.

One can see, that the maximum value itself is very high, about 10 times higher than the ultimate strength value. On the other hand, the minimum value can be quite small depending on the wire length. The average transverse stress is given by $\langle \tau_{xx} \rangle = \frac{G}{S}X' - E\frac{J}{S}X'''$. For small deflections, $|X|/\xi_L \ll 1$, it is in general smaller than the longitudinal one.

From the qualitative point of view it is evident that the maximal stress energy can be accumulated if the temperature rises sufficiently quickly. The temperature rise time must be shorter or comparable with the rise time of the instability. The most dramatic result might be expected if the wire is heated up to the temperature just slightly below the melting point. Then the current is switched off thus allowing the instability to develop without melting the material. On the other hand, if the current is low and, as a consequence, the temperature rise time is low too, then all the accumulated energy can be released at the onset of the

instability by the first mode which is becoming first unstable. This case corresponds to the lower limit of the estimated stress value τ_{zz}^{min} .

Thus, already now, from the linear analysis, it is obvious that many scenarios of the instability are possible. Dynamically, many modes can be excited simultaneously while the temperature T increases from T_0 up to the melting point T_{melt} . Even though the first mode becomes first unstable it might happen that further other modes play dominant role creating rather complex dynamical behaviour. Any particular pattern, of course, depends on temporal characteristics such as the ratio between instability increment and the temperature rise time.

5 Numerical results

Now, there are several further questions. What character will the instability have on the nonlinear stage? How high longitudinal and transverse stresses could be obtained in this situation? To answer these questions we solve the nonlinear equation (1) numerically.

5.1 Numerical algorithm

The numerical method of the solution of equation (1) with the boundary conditions (3) is based on the complete set of orthogonal functions (14).

By expanding any solution to (1) into the series of the functions $\{\mathcal{X}_i\}$, i.e $X = \sum_i A_i \mathcal{X}_i$, the partial differential equation turns into a system of ODEs with respect to time. They are

$$\sum_j B_{ij} \frac{d^2 A_j}{dt^2} + A_i \frac{\lambda_i^4}{2} + A_i \frac{\lambda_i^2}{2} \left\{ \beta_a (\tilde{l} - \tilde{l}_0 - \alpha[T(t) - T_0]) + \beta_B (0.14 + \ln(\lambda_i a / L)) \right\} = 0 \quad (31)$$

where the coefficients are $\beta_a = 4L^2/a^2$, $\beta_B = \frac{\mu_0 I^2 L^2}{4\pi E J}$. The symmetric matrix B_{ij} is given by $B_{ij} = \int_0^1 X_i X_j dz$. The length increment is $\tilde{l} - \tilde{l}_0 = \frac{1}{4} \sum_j (A_j^2 - A_j^{02}) \lambda_j^2$. The functions X , X_0 and the variable z have been normalised on L and t has been normalised by $t_0 = \sqrt{\frac{\rho S}{E J}} L^2$. In the numerical simulations, the infinite series have been truncated at the maximal unstable mode defined by (28).

5.2 Flexural vibrations of initially straight wires

In the case of initially straight wires the initial conditions are $A_i(0) = 0$. To excite the instability one needs to seed some initial noise level. To simulate noise present an additional fluctuation force in the equation (1), $\delta F = \delta F_0 \delta f(t) \sum_i \exp(-\xi_i^2/\xi_1^2) \mathcal{X}_i$, has been added, with $\delta F_0 = 4 \times 10^{-4}$ newton. The function $-1 < \delta f(t) < 1$ has been calculated by means of a random number generator at each step of calculations over time. This force can give rise to deflection of an aluminium wire with $L = 1$ m and $a = 0.6$ mm from a straight line by approximately $X \sim 0.1 a$.

The current profile in the simulations has been taken in the form $I(t) = I_0 \sinh(t/t_0)/\cosh(t/t_0)$, where t_0 is the current rise time. In all runs $t_0 = 30 \mu\text{sec}$. This time is about twice as high as the skin time for aluminium wires with $a = 0.6$ mm, $t_{\text{skin}} = a^2 \sigma \mu_0 \simeq 17 \mu\text{sec}$. We also kept $T_0 = 300^\circ \text{K}$ and calculations stopped once the temperature had reached the melting point $T = T_{\text{melt}}$. We designated this moment by $t = t_e$.

We have performed simulations for different conditions: different wire lengths, different currents and different wire materials. All the sets used are presented in Table I.

As the first example, let's consider a short aluminium wire carrying 5 kA current, case [A]. For these parameters from the linear analysis one would expect a few unstable modes to develop, $i_{\text{lim}} = 6$. The results obtained are presented in Fig.1. We have plotted in the first two frames the deflection X as a function of z and the spectrum $\langle A(t)_i^2 \rangle$ both taken at $t = t_e$. In the last two frames, we have plotted the longitudinal τ_{zz} and transverse $\langle \tau_{xx} \rangle$ stress components as functions of time. The spectrum has been calculated by means of averaging over time around $t = t_e$, i.e. $\langle A(t_e)_i^2 \rangle = \int_{t_e - \Delta}^{t_e} A(t)_i^2 dt$, where Δ is chosen to be greater than the period of nonlinear vibrations. Both the spectrum, Fig.1b and the wire shape, in the form being close to a simple arc, Fig.1a, show that the first mode dominates during the nonlinear stage of the instability. Temporal behaviour of the longitudinal and transverse stress components demonstrates developed nonlinear flexural vibrations, Fig.1c and Fig.1d. The appearance of the instability is clearly seen at $t \simeq 900 \mu\text{sec}$ in both figures. The observed longitudinal stress has both compressive and tensile components. The instability appeared

after strong compression, the maximal compressive stress being 429 MPa. The maximal tensile longitudinal stress is amounting to $\tau_{zz} \simeq 244$ MPa. This value is well above the ultimate stress value for aluminium. The observed transverse stress, as has been expected, is lower then the longitudinal one, $\langle \tau_{xx} \rangle \simeq 55$ MPa.

Let's consider now a longer wire, case [B]. This case is relevant to the conditions of the Graneau's experiments [4]. One might expect, in accordance with our qualitative analysis, more active modes in the instability spectrum to develop with respect to the previous case, $i_{lim} = 129$. Indeed, from Fig.2a and Fig.2b one can observe that the spectrum becomes very rich with the major contribution from mode $n = 27$ at the melting point. The tensile longitudinal and transverse stresses are amounting to $\tau_{zz} = 122$ MPa and $\langle \tau_{xx} \rangle = 92$ MPa in this case, see Fig.2c and Fig.2d. Both of them are well above the ultimate strength of aluminium. Thus, one might expect the first wire break to appear just after buckling occurred, at $t = 1000 \mu\text{sec}$.

Let's investigate now the effect of variations of current. In case [C], which is a replica of case [B] but with lower current, two modes $n = 5$ and $n = 7$ become dominant, Fig.3a. This fact indicates, if we compare two spectra in cases [B] and [C], that the main channel of the accumulated energy to release is going now through the modes with lower numbers. Thus, one would anticipate a lower accumulated stress according to our qualitative stress analysis. Indeed, we have observed that both tensile longitudinal and transverse stresses reduced to $\tau_{zz} = 70$ MPa and $\langle \tau_{xx} \rangle = 23$ MPa, Fig.3b and Fig.3c.

On the other hand, an increase of the current leads to higher resultant tensile stress value. In case [D] which is similar to set [B] but with a higher current, the longitudinal tensile stress is $\tau_{zz} \simeq 233$ MPa in maximum, Fig.4. It should be noted that because of faster heating the preliminary compression before the instability developed is much more stronger, namely 851 MPa, and the instability occurred just before the melting point. It appears that at higher current the wire will be molten before the buckling occurs.

Let's consider now the Nasilovski's experiment with a long copper wire, case [E]. This experiment has been carried out at quite a low current $I = 500$ A in comparison with the

all previously considered cases. As a result, one might expect low stress values compared to previous cases. Also, a few first modes must be dominant. Indeed, that is just the case, see Fig.5a. The observed values of stress indeed become quite low. The longitudinal stress is reaching $\tau_{zz} \simeq 27$ MPa in maximum, Fig.5b, while the transverse stress is just about 4 MPa. It means that the wire can be broken only if it was heated up enough.

5.3 Flexural vibrations of initially bent wires

In the above, we considered somewhat idealised situation, when the undeformed wire had the shape of a straight rod. In reality, the wire might have had initially any form. For instance, in the case of horizontal positioning of the wire it might be bent by gravitational force. Once the initial dislocation becomes grater than the radius, the character of the instability changes as has been discussed. Indeed, if $X_0 \neq 0$ the initial state is unstable from the beginning. But, if the temperature risetime is shorter than the period of flexural vibrations then those modes which contribute into $X_0 = \sum_i A_i^0 \mathcal{X}_i$ can be excited directly. Moreover, buckling on the other modes is still possible. To estimate the stresses developed simulations for case [B] have been performed but with initial conditions given by $X_0 = A_1^0 \mathcal{X}_1$ with $A_1^0 = 20a$. That is, the wire was initially shaped like the first mode of the set (14). The choice of the amplitude A_1^0 follows from estimations for a horizontally positioned wire of this length. The wire in this case has a form $X_0 = \frac{qz^2(z-L)^2}{24EJ}$, see the problem in [10] page 93, q being the wire weight per unit length. Thus, the maximal displacement is expected to be $X_{0\max} \sim 18a$.

The results of simulations are shown in Fig.6. As before, one can see developed nonlinear vibrations. The regular character of the vibrations points out to the fact that only one single mode $i = 1$ is active in this case. This means that buckling on the other mode didn't occur. The amplitude of tensile longitudinal stress is amounting for this particular case to $\tau_{zz} \simeq 50$ MPa. So, a sufficiently heated wire can be broken in this case as well.

Conclusions

When an electric current passes through a thin metal wire with clamped ends, flexural elastic stress waves are induced owing to the Joule heating and the electromagnetic force. The Joule heating leads to thermal expansion of the wire material, which is the dominant mechanism of the excitation of vibrations. Under realistic experimental conditions the electromagnetic force is of minor importance.

Flexural vibrations in an initially straight wire may be excited as a result of the buckling instability. The energy accumulated in the wire during the initial stage in the form of a compressive stress is suddenly released. As a result, high tensile stress appears, which is sufficiently high to cause the fracture of the wire within 1 ms for all the cases considered. The number of modes of the instability that are excited depends on the current magnitude and wire length. Depending on these parameters it is possible to excite just a single mode, which has a form of an arch, or actually any number of modes.

If a wire is slightly curved, which is a more realistic case than that of the straight wire, the buckling instability is still possible. The amplitude of modes, that are initially present in the curved wire, grows. The other modes can still be excited in a rapidly heated wire owing to buckling instability. The magnitude of tensile stress induced in a curved wire is clearly lower, but is still sufficient to induce a wire fracture on a millisecond timescale.

Three-dimensional effects, which may be induced by the external circuit, suspensions at the clamped ends, imperfections of the wire cross-section or a wire material, will increase the magnitude of tensile stress. These effects will lead to the coupling between flexural, longitudinal, and torsional modes. This study is beyond the scope of the present paper.

The experimental evidence, in general, is supportive of the mechanism described above. However, no direct comparison is possible, since previous experiments were of exploratory nature.

The model developed favours the view that the phenomenon of the wire fragmentation in the solid state can be explained without resorting to controversial Ampère-Neumann electrodynamics.

Acknowledgements

This work has been supported by Engineering and Physical Sciences Research Council grant No. GR/M07403. The authors are grateful to Prof. J. Allen and Dr. D. Wall for useful discussions. A. Lukyanov would like to express his gratitude to O.V. Umnova for support.

References

- [1] J. Nasilovski, Unduloids and striated disintegration of wires *Exploding wires* 1964, v.3, ed. W.G. Chase and H.K. Moore, (New York: Plenum), p.295.
- [2] P. Graneau, Longitudinal magnet forces? *J. Appl. Phys.* 1984, v.55, p.2598.
- [3] P. Graneau, Ampere tension in electric conductors, *IEEE Trans. Magn.*, 1984, v.20, p.444.
- [4] P. Graneau, Wire explosions, *Phys. Lett. A*, 1987, v.120, p.77.
- [5] P. Graneau, Ampere-Neumann Electrodynamics of Metals, 1994, Palm Harbor: Hadronic.
- [6] J. S. Hong, Electromagnetic forces in flexible systems, DPhil Thesis University of Oxford, 1994.
- [7] S. Molokov, J. E. Allen, The fragmentation of wires carrying electric current, *J. Phys. D*, 1997, v.30, p.3131.
- [8] J.G. Ternan, Stresses in rapidly heated conductors, *Phys. Lett. A*, 1986, v.115, p.230.
- [9] Smithells Metals Reference Book 7th ed., editors E.A. Brandes and G.B. Brook, London, Butterworth 1998.
- [10] L.D. Landau, E.M. Lifshitz, *Theory of elasticity*, 1970, (Oxford: Pergamon Press), p.89.
- [11] W.B. Thompson, "An Introduction to Plasma Physics", Pergamon Press, 1964, p.107.

- [12] S. Chattopadhyay, F. Moon, Magnetoelastic buckling and vibration of a rod carrying electric current, *J. Appl. Mech.*, 1975, December, p.809.
- [13] L.D. Landau, E.M. Lifshitz, *Electrodynamics of Continuous Media*, 1984, (Oxford: Pergamon Press), p.123.
- [14] M.A. Leontovich and V.D. Shafranov, "The stability of a flexible conductor in a longitudinal magnetic field". *Plasma physics and the problem of thermonuclear fusion reactions*, v.1, Pergamon Press, 1961.
- [15] W.F. Chen and T. Atsuta, *Theory of Beam-Columns*, V.1. 1976, McGraw-Hill, Inc.

Captions

Fig.1a The wire displacement X/L as a function of z/L , case [A].

Fig.1b The spectrum of the wire vibrations at the melting point $\langle A_i^2 \rangle$ as a function of mode number i , case [A].

Fig.1c The longitudinal stress τ_{zz} as a function of time, case [A].

Fig.1d The transverse stress $\langle \tau_{xx} \rangle$ as a function of time at $z/L = 0.9$ at $z/L = 0.9$, case [A].

Fig.2a The wire displacement X/L as a function of z/L , case [B].

Fig.2b The spectrum of the wire vibrations at the melting point $\langle A_i^2 \rangle$ as a function of mode number i , case [B].

Fig.2c The longitudinal stress τ_{zz} as a function of time, case [B].

Fig.2d The transverse stress $\langle \tau_{xx} \rangle$ as a function of time at $z/L = 0.9$, case [B].

Fig.3a The spectrum of the wire vibrations at the melting point $\langle A_i^2 \rangle$ as a function of mode number i , case [C].

Fig.3b The longitudinal stress τ_{zz} as a function of time, case [C].

Fig.3c The transverse stress $\langle \tau_{xx} \rangle$ as a function of time at $z/L = 0.9$, case [C].

Fig.4 The longitudinal stress τ_{zz} as a function of time, case [D].

Fig.5a The spectrum of the wire vibrations at the melting point $\langle A_i^2 \rangle$ as a function of mode number i , case [E].

Fig.5b The longitudinal stress τ_{zz} as a function of time, case [E].

Fig.6 Flexural vibrations of an initially bent wire, longitudinal stress as a function of time. $X_0 = A_1^0 \mathcal{X}_1$, $A_1^0 = 20a$. The wire and current parameters are relevant for case [B].

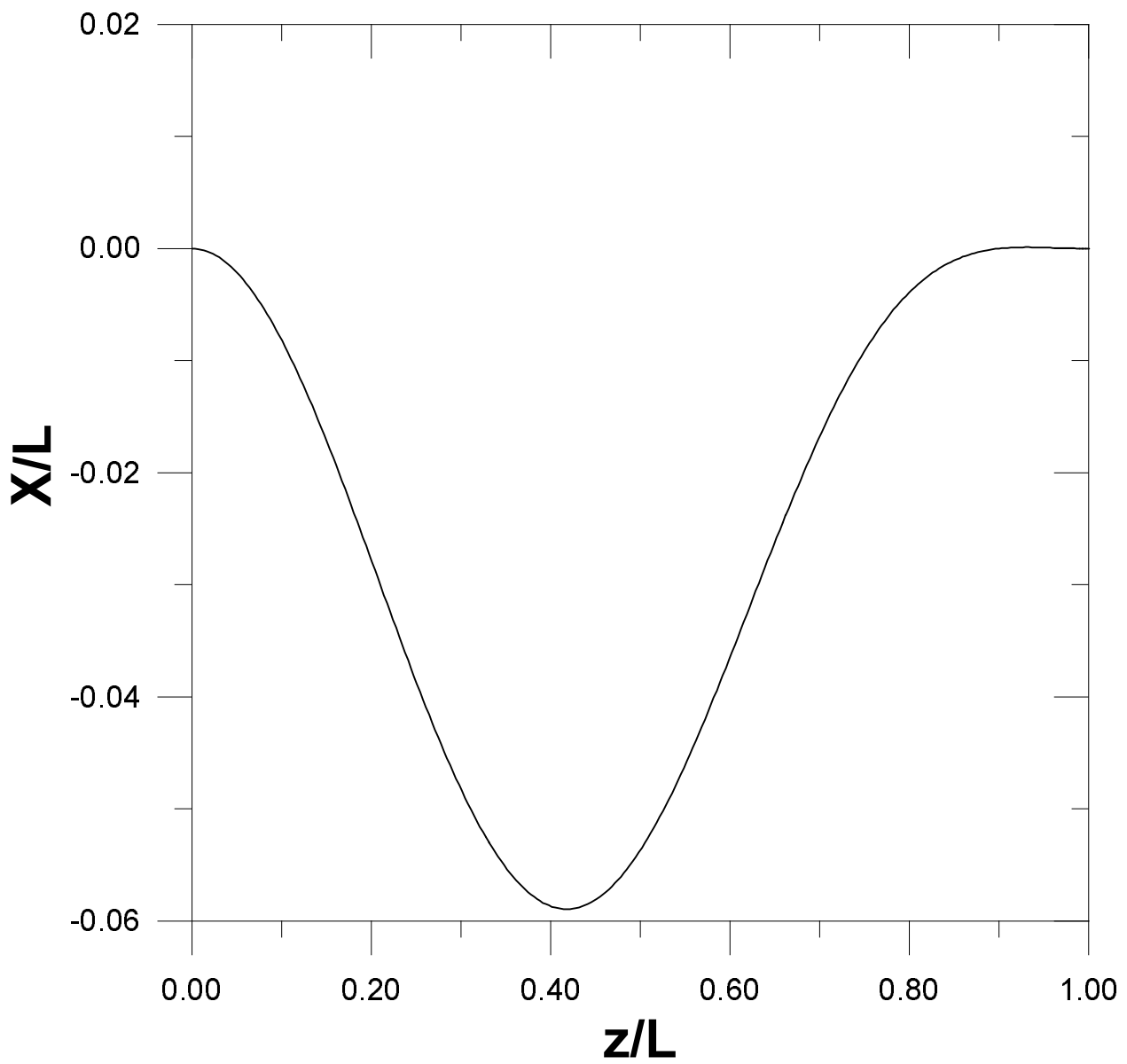


Fig. 1a

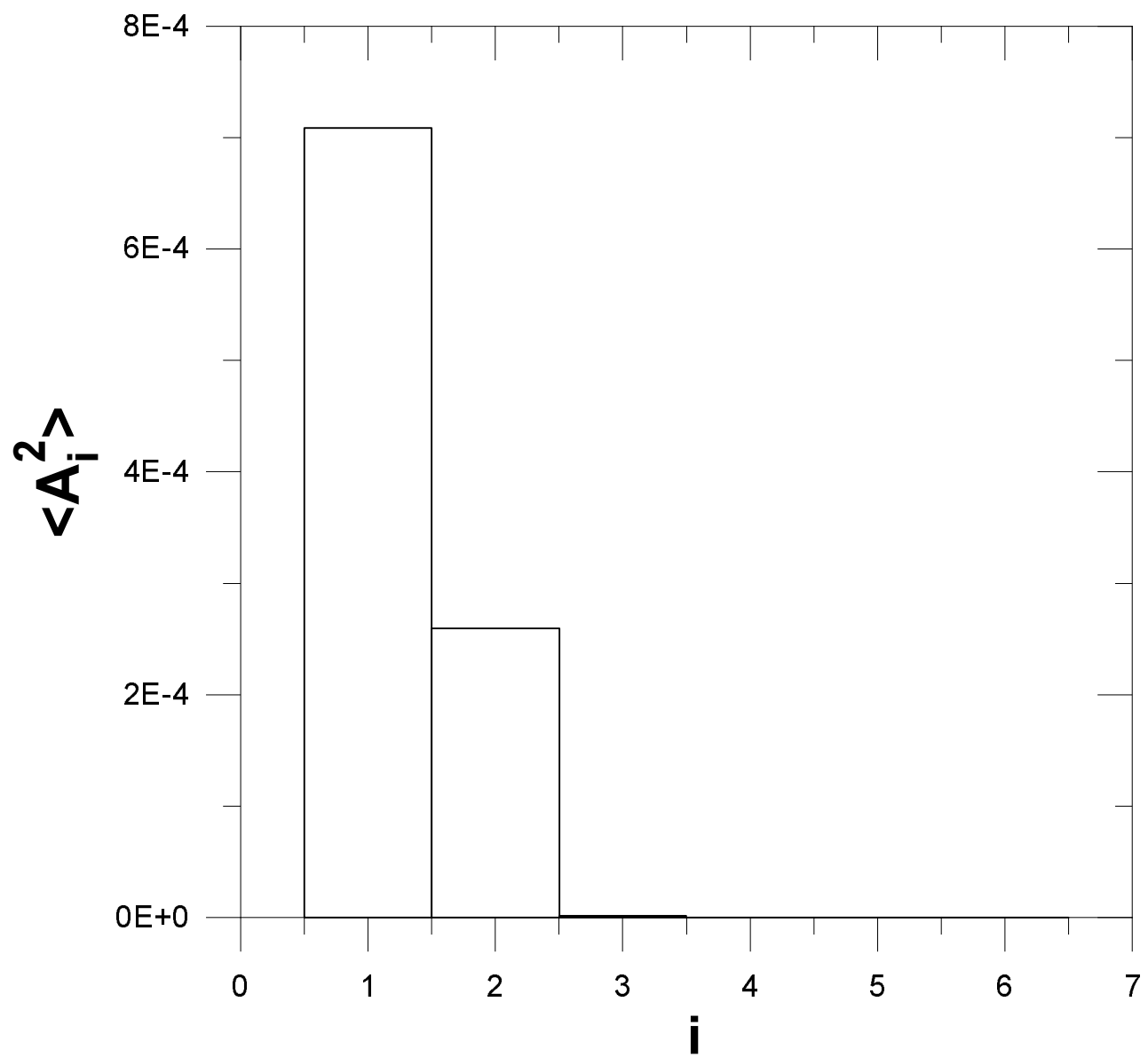


Fig.1b

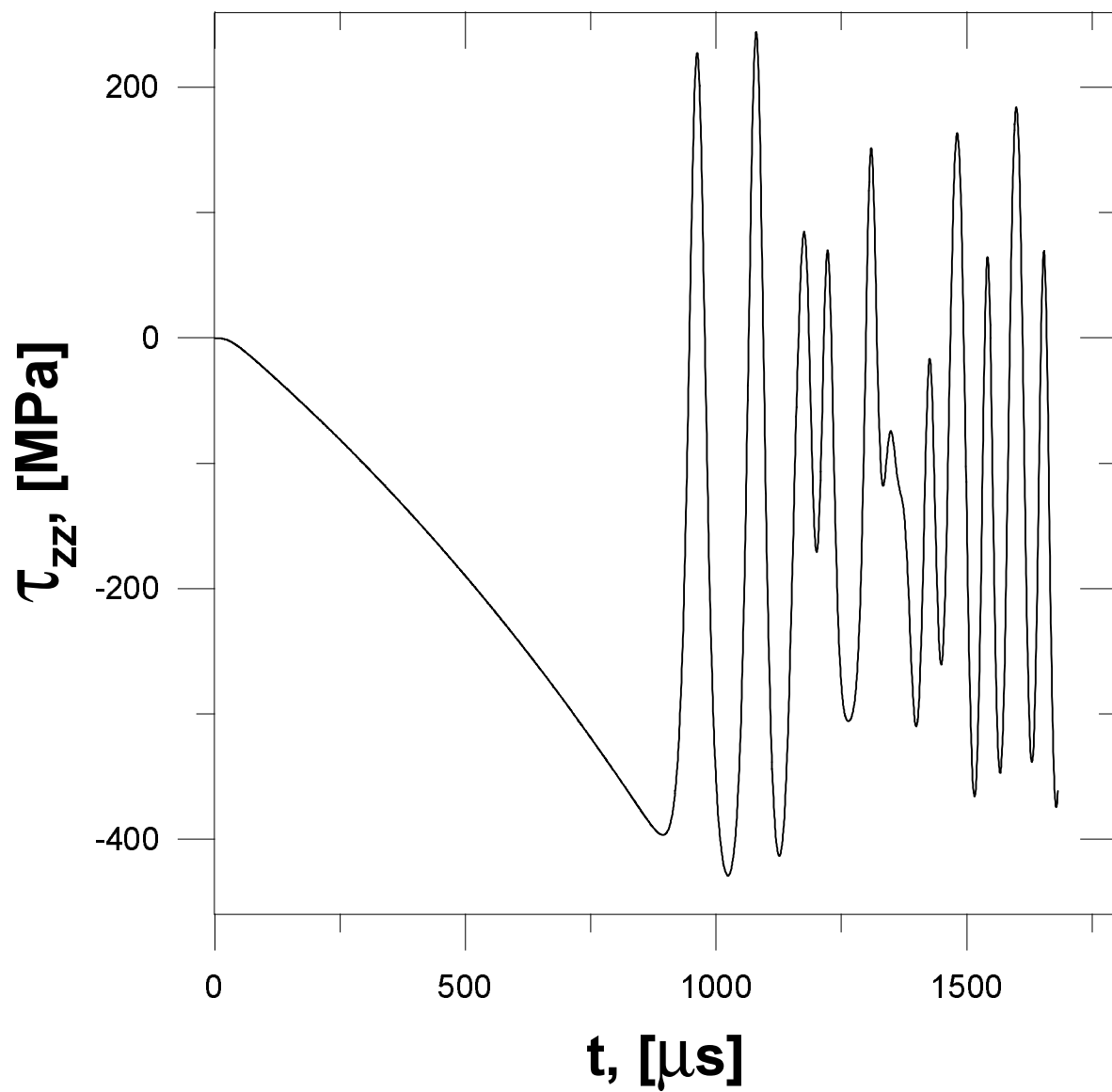


Fig. 1c

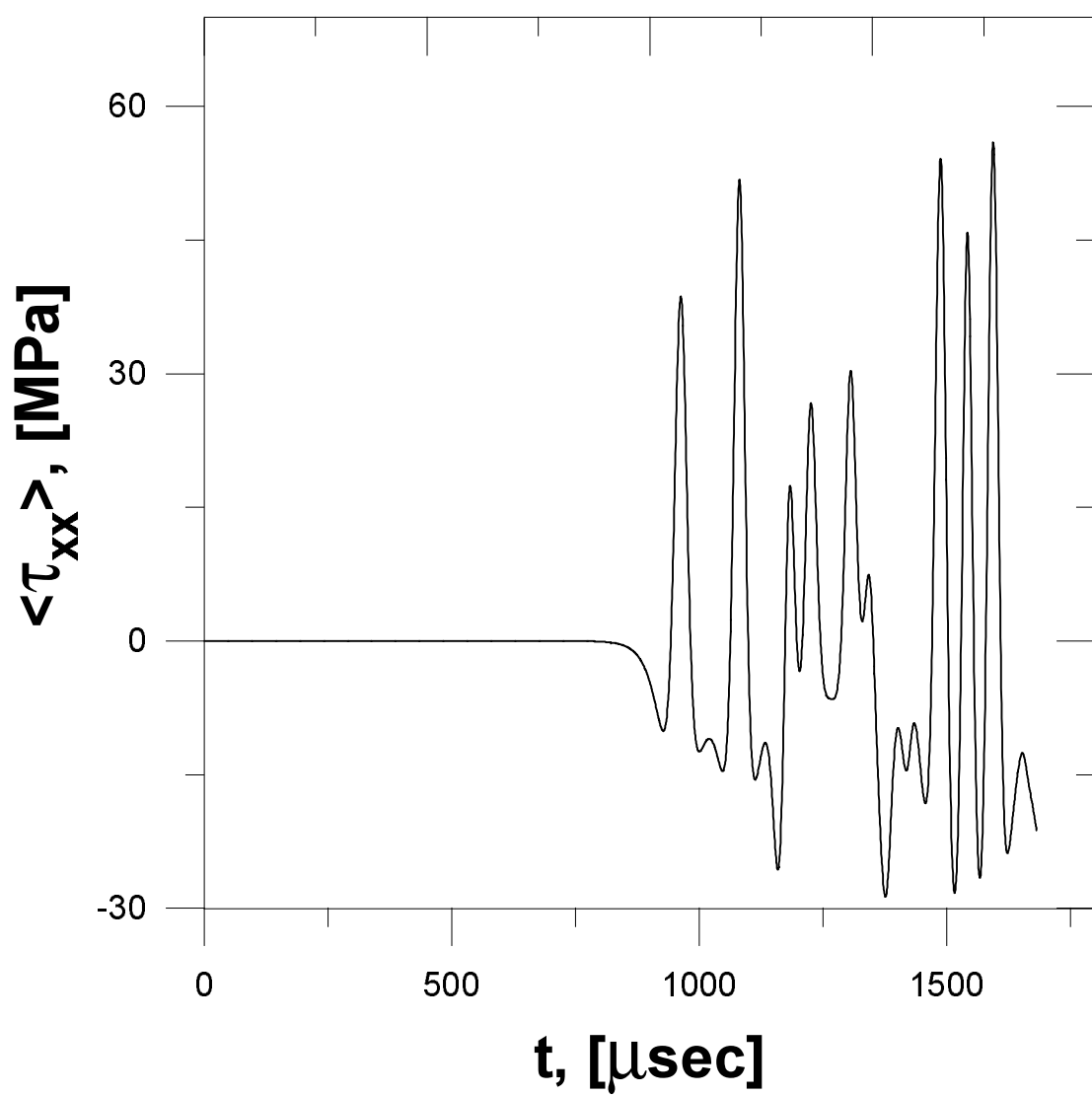


Fig.1d

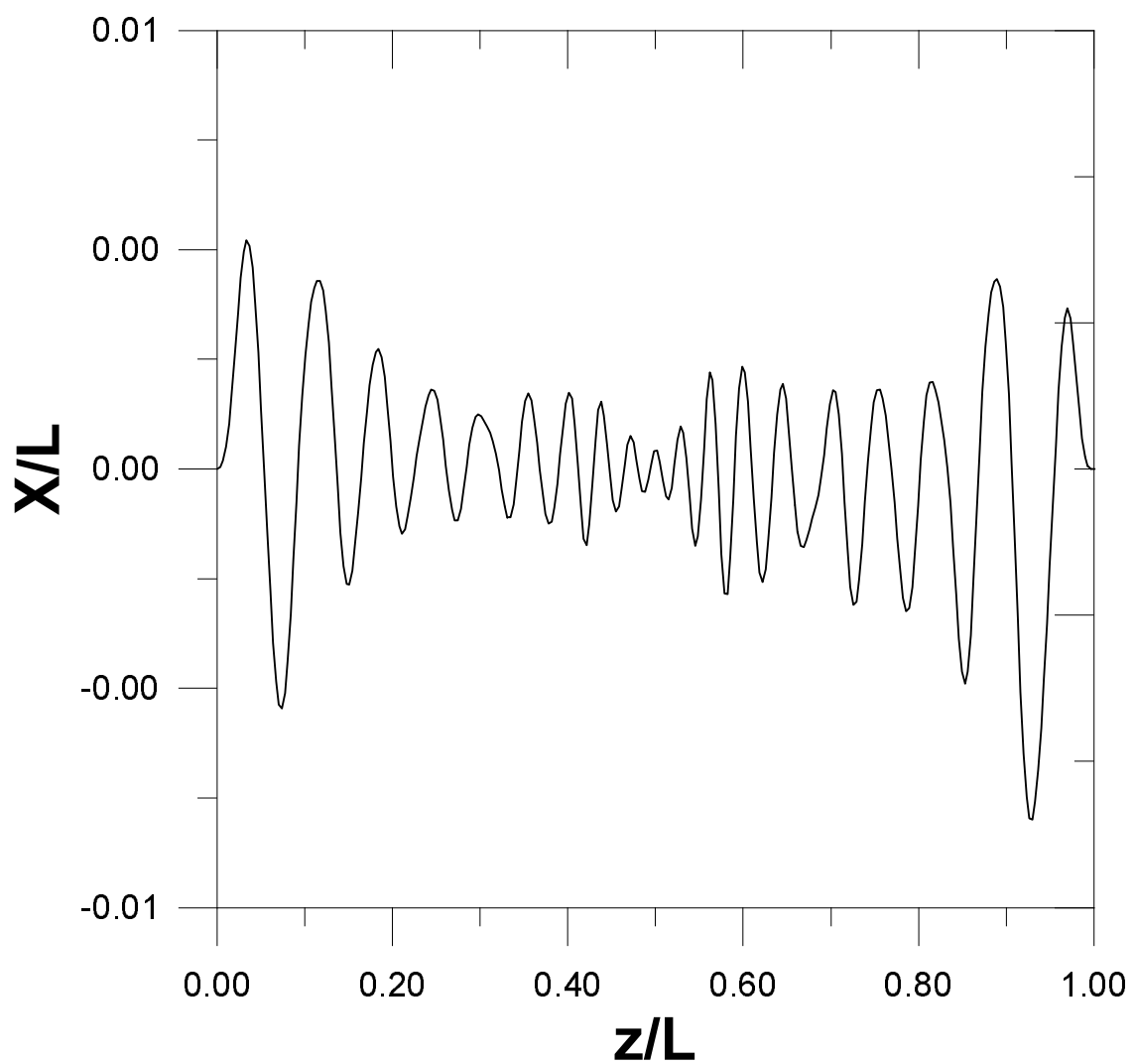


Fig.2a

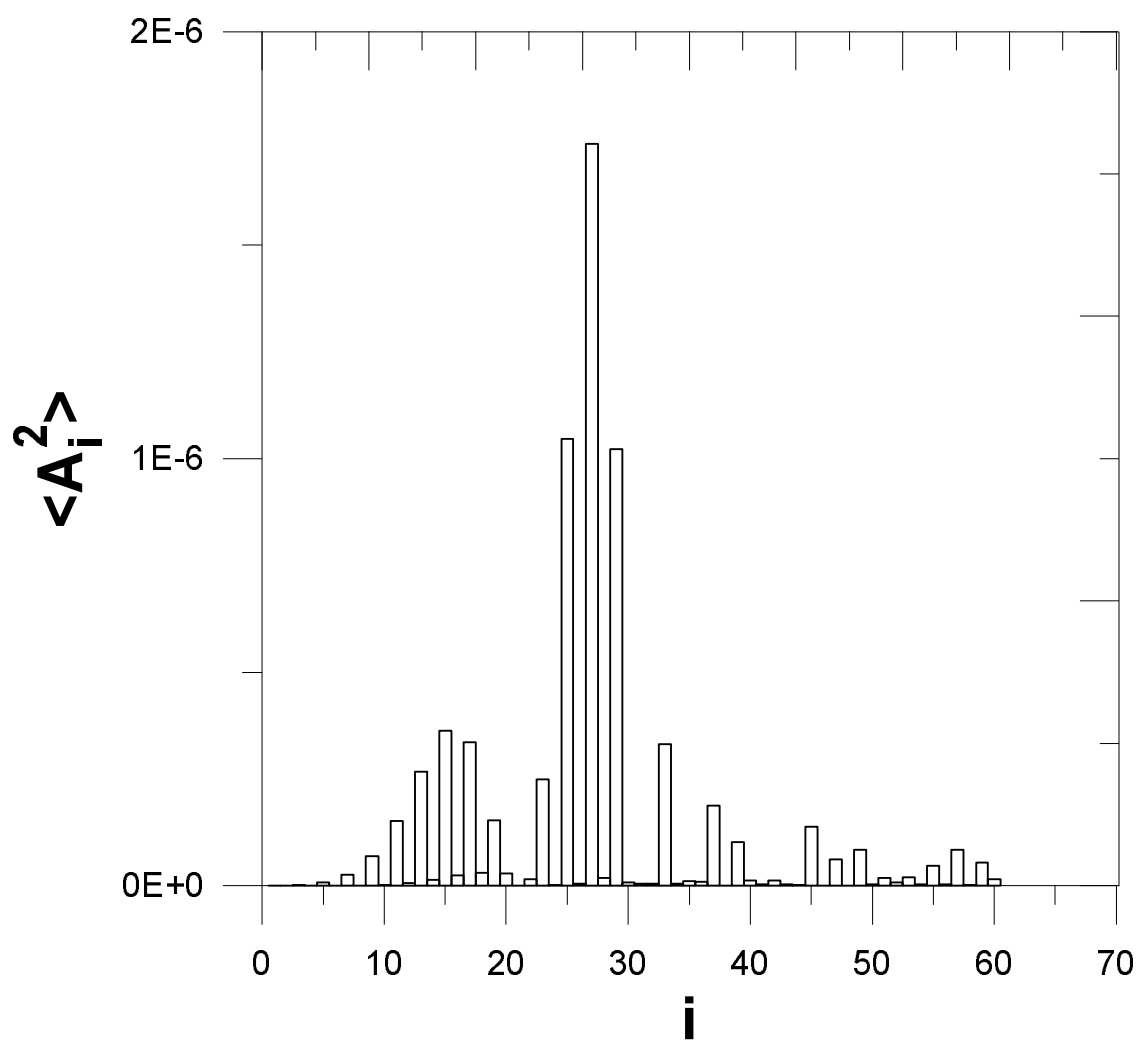


Fig.2b

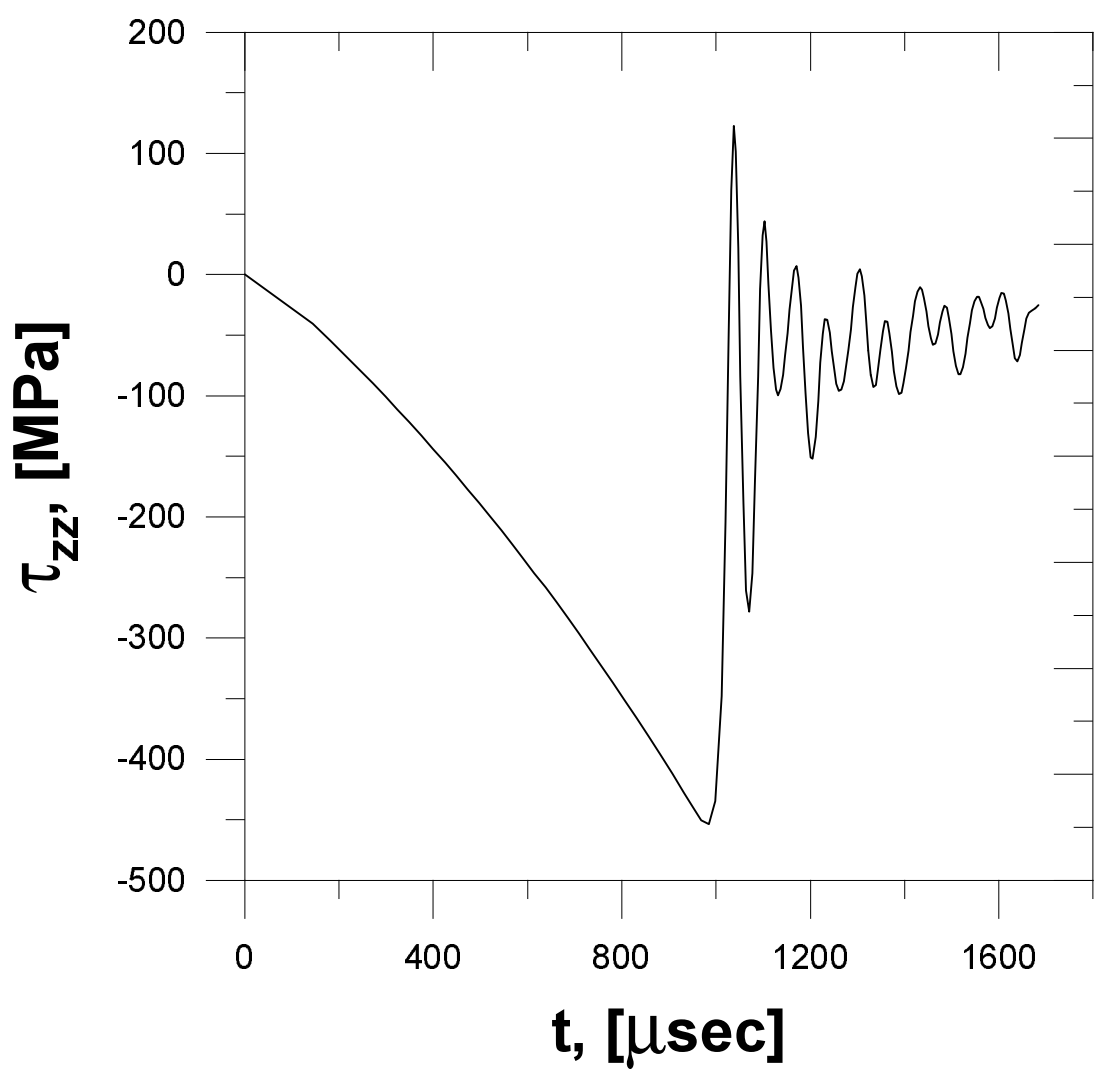


Fig.2c

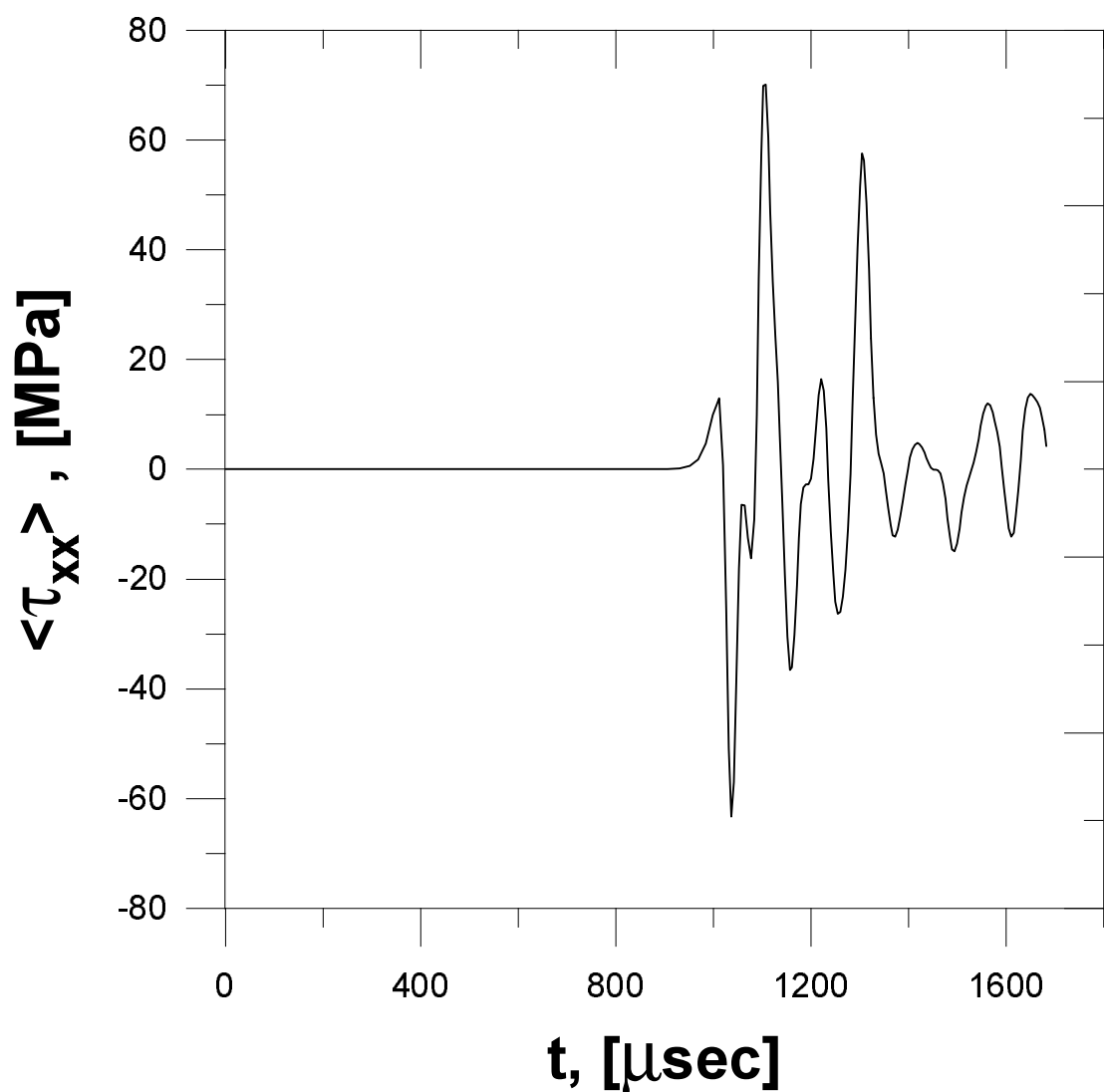


Fig.2d

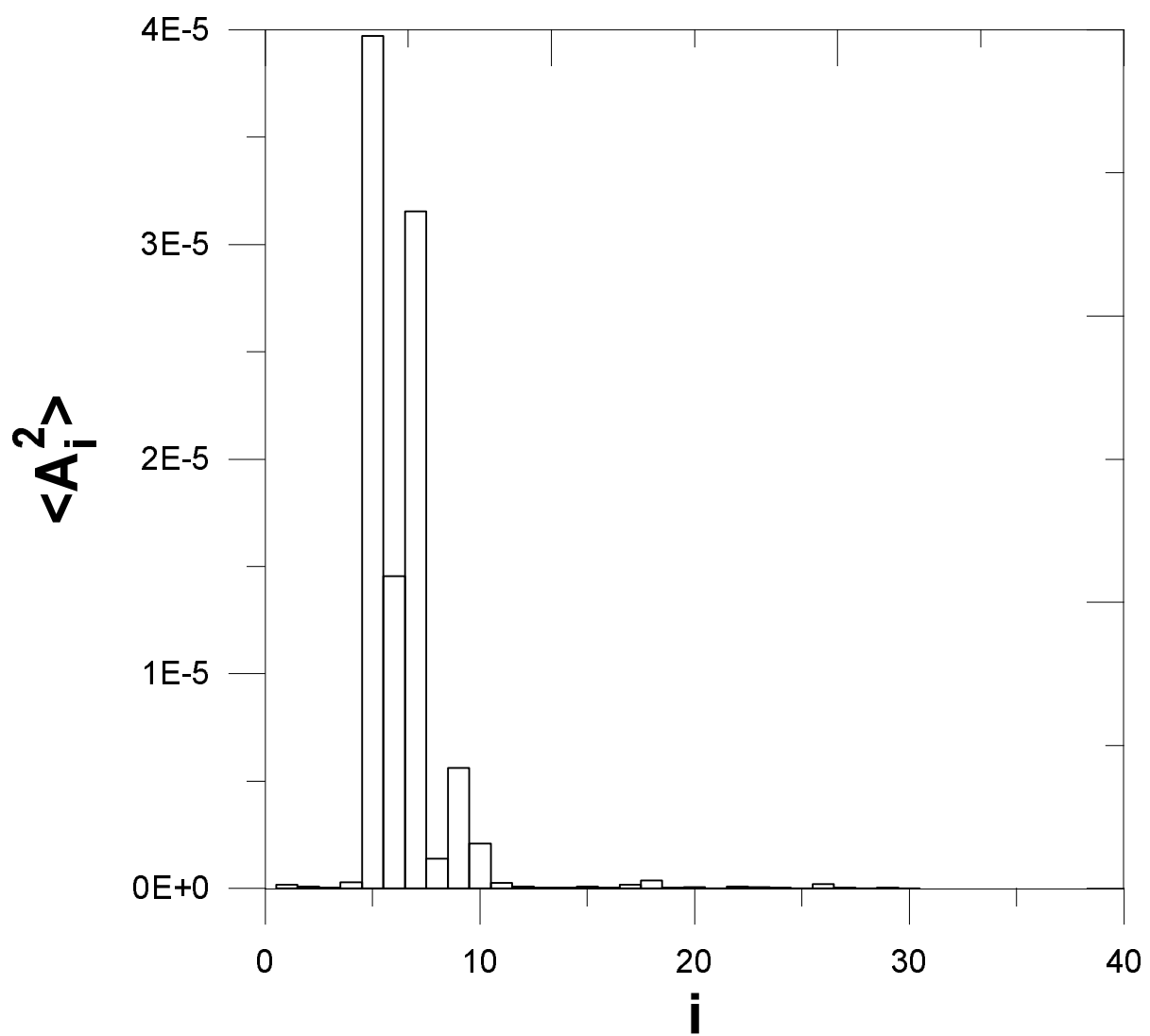


Fig.3a

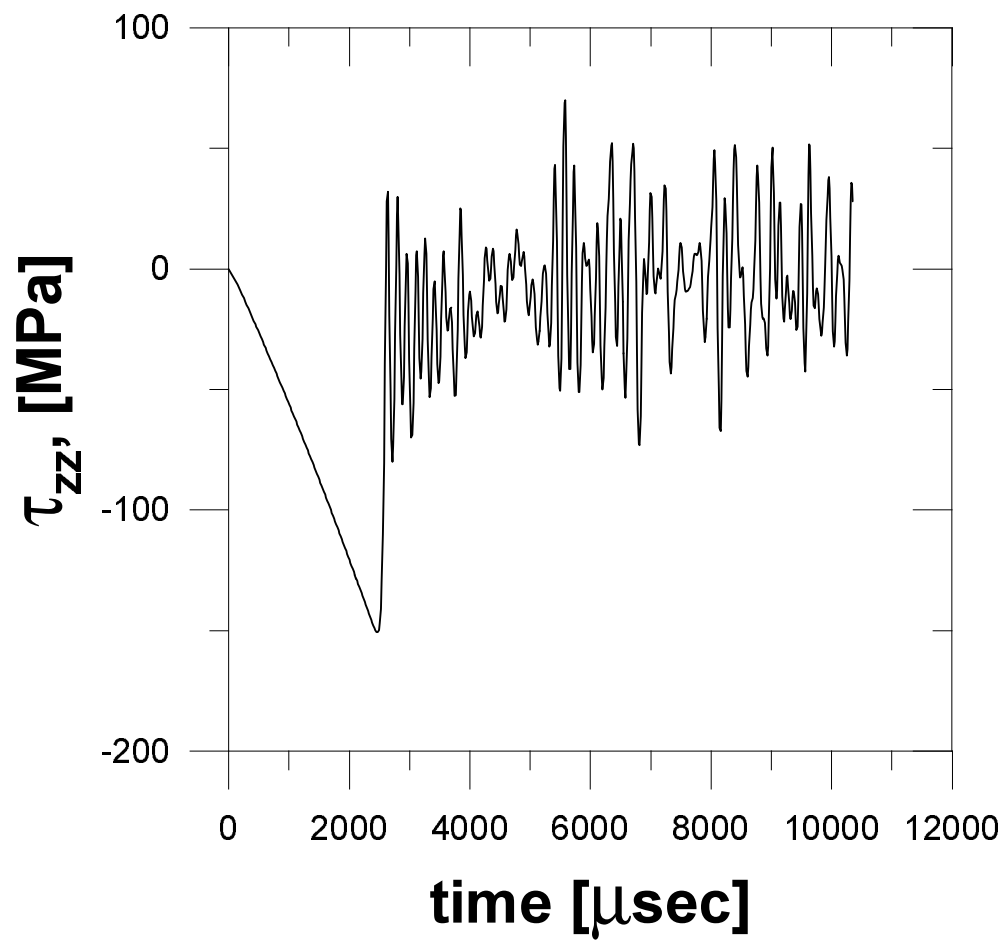


Fig.3b

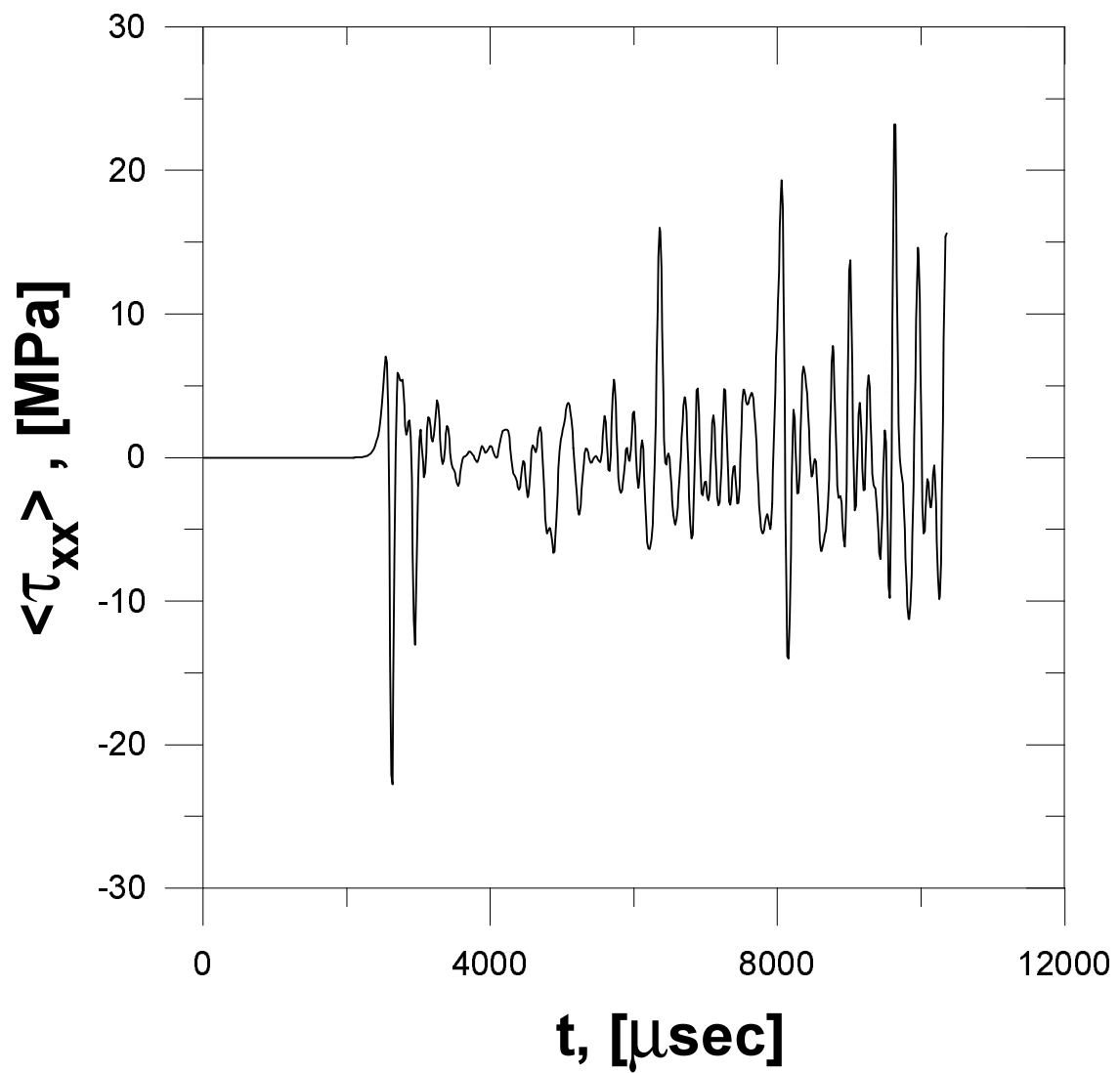


Fig.3c

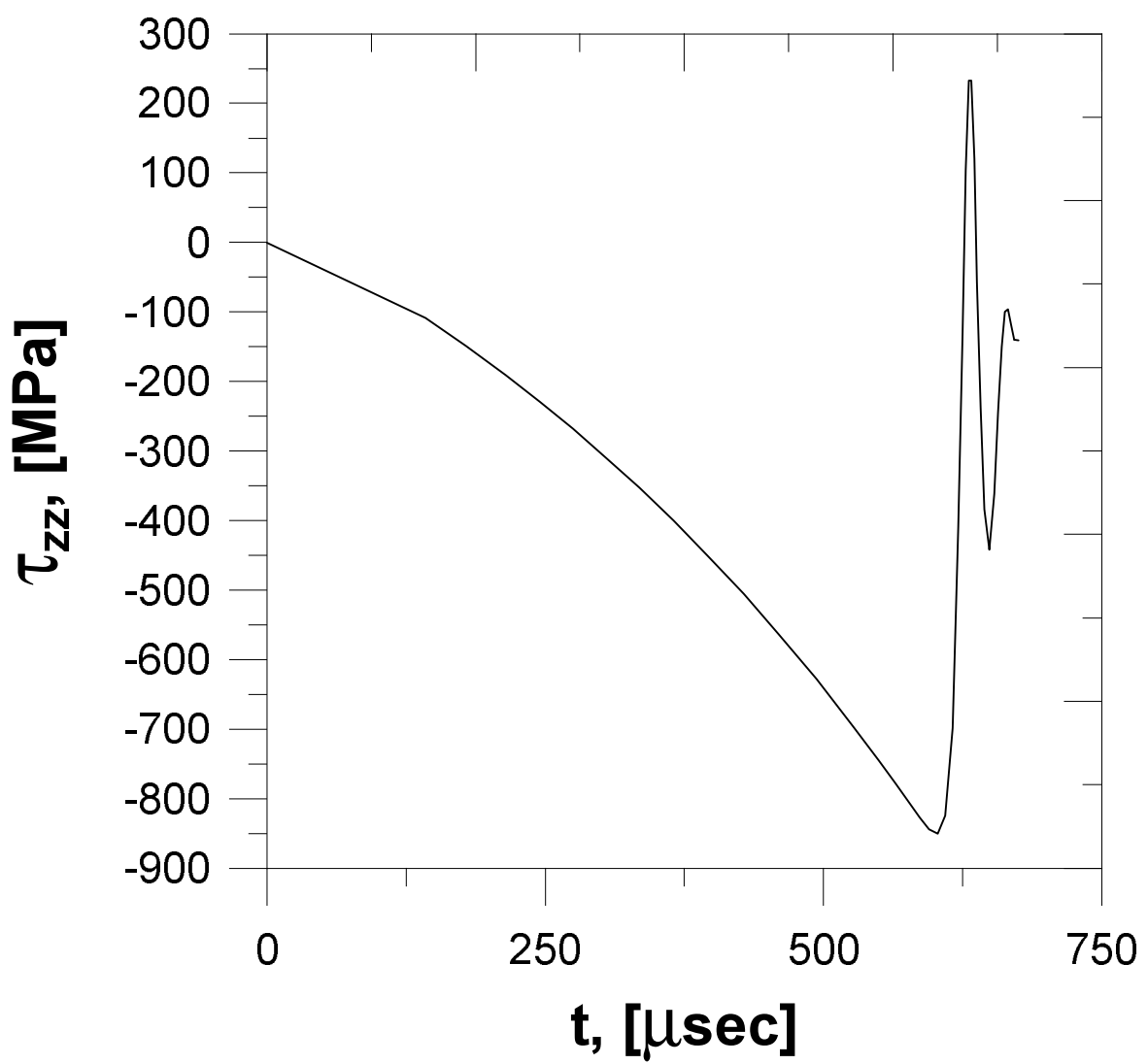


Fig.4

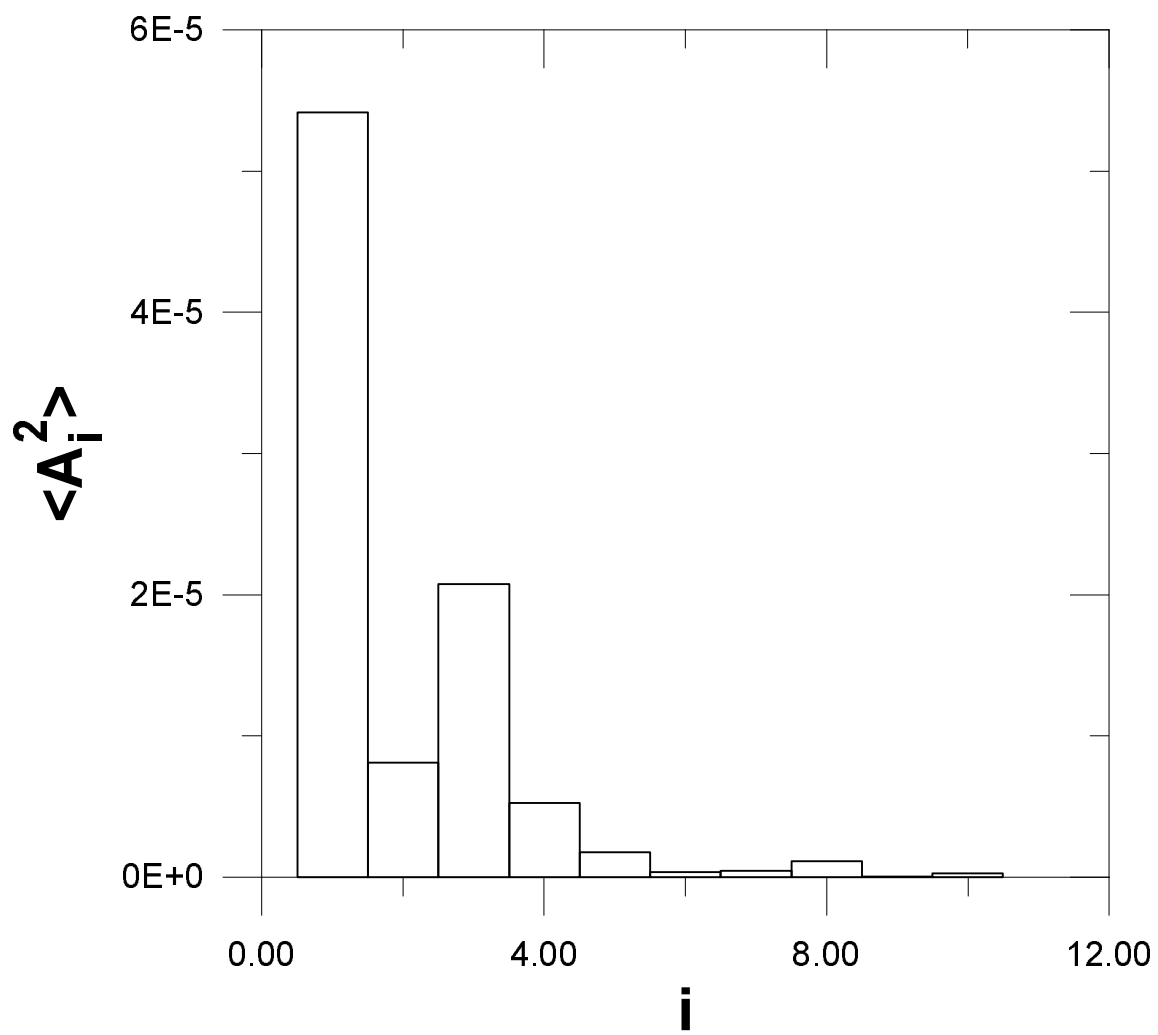


Fig.5a

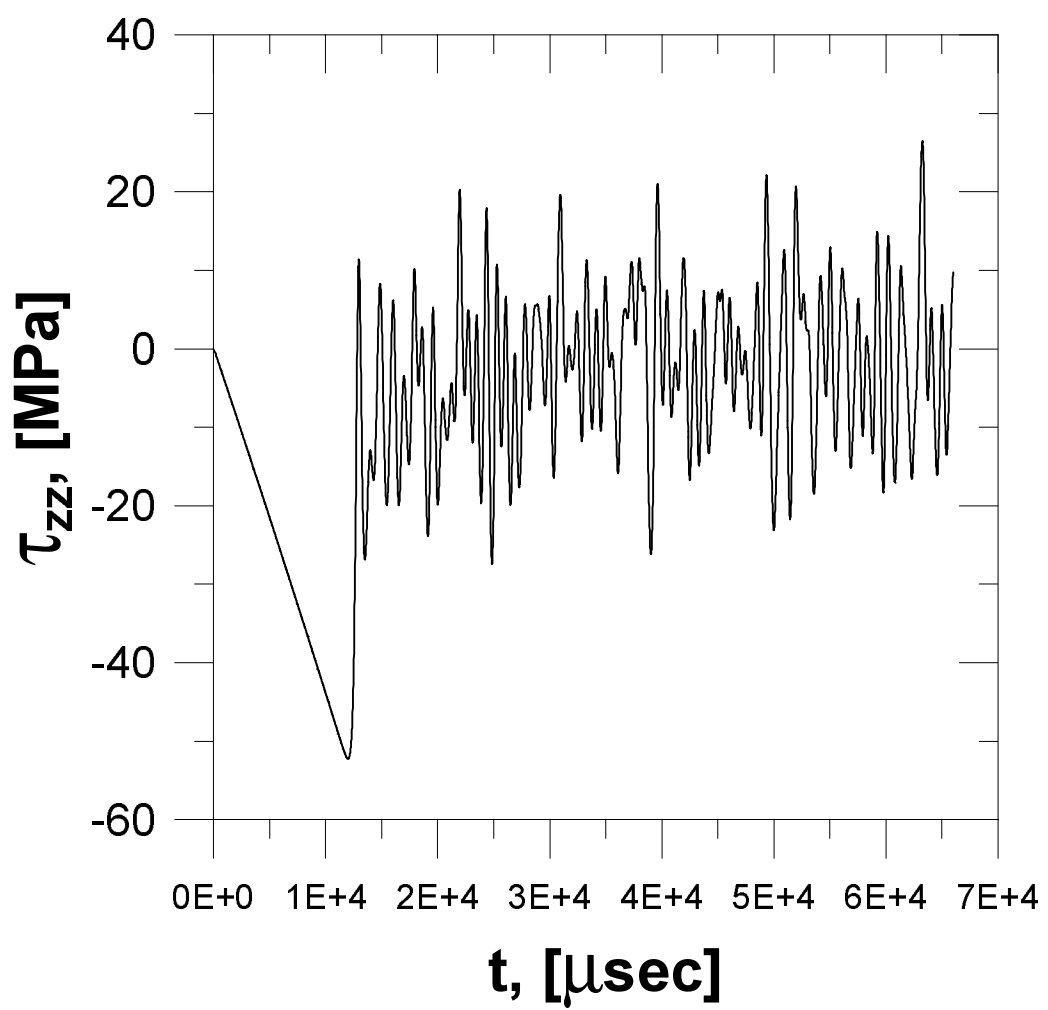


Fig.5b

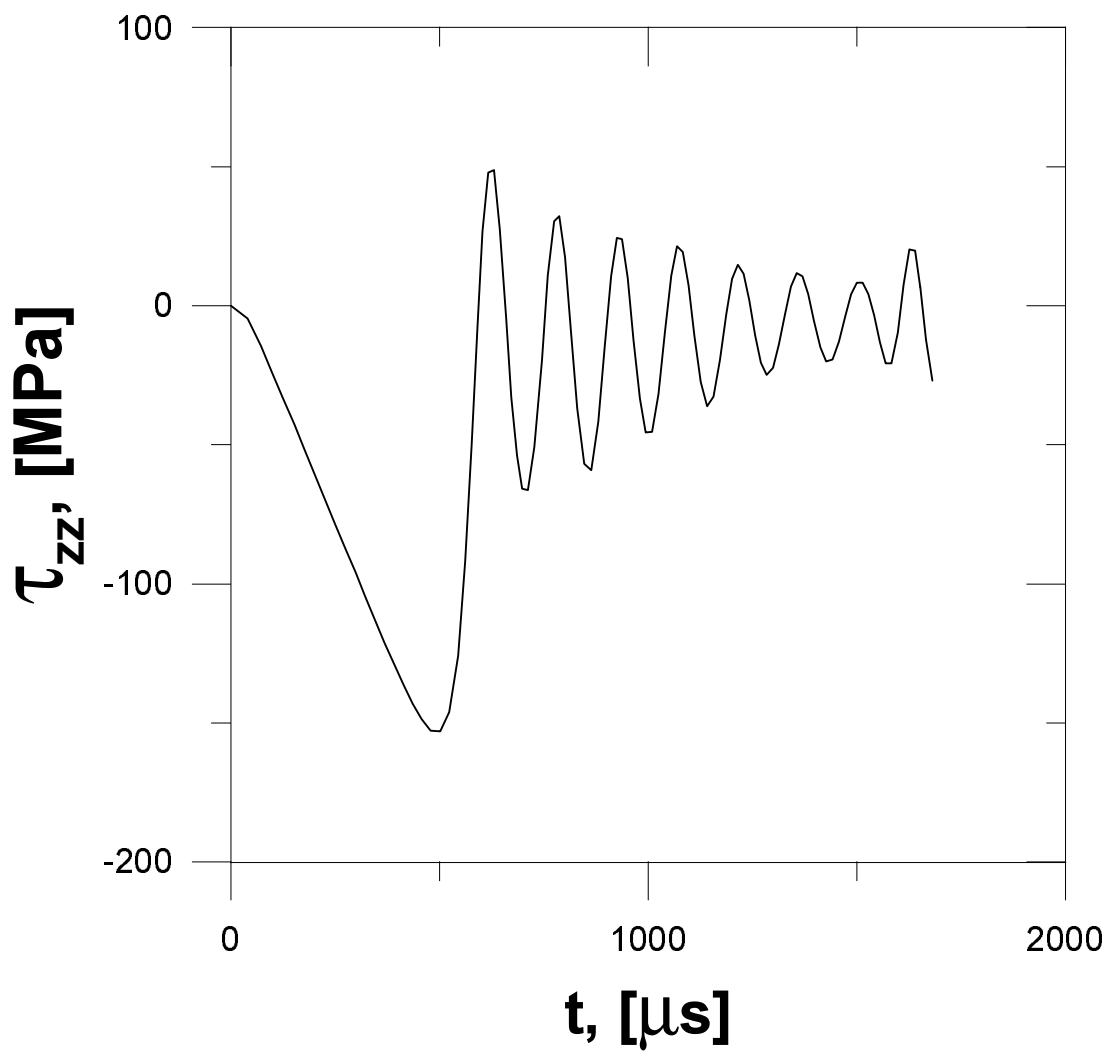


Fig.6